

QSAR, in silico docking and in vitro evaluation of chalcone derivatives as potential inhibitors for H1N1 virus neuraminidase

Marzieh Yaeghoobi^{1,2} · Neni Frimayanti^{1,2} · Chin Fei Chee^{1,2} · Kusaira K. Ikram³ · Belal O. Najjar³ · Sharifuddin M. Zain¹ · Zanariah Abdullah¹ · Habibah A. Wahab³ · Noorsaadah Abd. Rahman^{1,2}

Received: 8 April 2015 / Accepted: 27 June 2016
© Springer Science+Business Media New York 2016

Abstract Thirty three chalcones were synthesized and tested on viral H1N1 neuraminidase activity by using MUNANA assay [2'-(4-methylumbelliferyl)- α -D-N-acetylneuraminic acid] assay with DANA (2,3-didehydro-2-deoxy-N-acetylneuraminic acid) was used as standard. 2D and 3D-quantitative structure–activity relationship models have been successfully developed with a good correlative and predictive ability for quantitative structure–activity relationships of these chalcone derivatives. Result from the 2D-quantitative structure–activity relationship model indicates that electrostatic parameter enhanced bioactivity of the chalcones while steric substituents diminished their potency as H1N1 neuraminidase inhibitors. 3D-quantitative structure–activity relationship model showed the importance of the position of the hydroxyl group in chalcone derivatives which can influence on hydrophobicity, hydrogen bond donor and aromatic ring features that enhance the biological activity. Finally, docking studies showed that chalcones **MC8** and **MC16** with low C docker interaction energies and higher numbers of hydrogen bonding have better inhibitory activity against viral H1N1 neuraminidase.

Keywords Neuraminidase · Chalcone · Pharmacophore · 2D-QSAR · 3D-QSAR

Introduction

Influenza virus belongs to the orthomyxoviridae, a family of RNA viruses which can cause infection in birds and mammalian cells with the help of hemagglutinin (H) and neuraminidase (NA) of the influenza virus. Neuraminidase is involved in the initiation of the influenza infection by promoting the release of the virus from the host cell. This enzyme is a crucial part of influenza replication. Thus, finding suitable inhibitors to block the function of NA is possibly an effective way to restrain influenza (Babu et al., 2000).

In the last decade, a number of investigations have been conducted on phytomedicines for their potential as neuraminidase inhibitor. Flavonoids, especially, are considered promising compounds and are widely found in traditional herb based medicines for influenza. For example, a series of flavonoids isolated from *Sophoraflavescens*, *Glycyrrhizauralensis*, *cadraniatricuspidata* and *Rhodio-larosea* were found to show moderate activities for NA inhibition (Jeong et al., 2009; Ryu et al., 2008, 2009, 2010). However, most work have been conducted on naturally occurring flavonoids, and amongst all the subtypes of flavonoids studied, chalcones have not been extensively investigated for their potency as NA inhibitors (Ryu et al., 2008, 2009; Gao et al., 2011; Mercader and Pomilio, 2010). Thus far, there is no report on quantitative structure–activity relationship for the chalcones as NA inhibitors. This study was conducted to investigate quantitative structure–activity

Electronic supplementary material The online version of this article (doi:10.1007/s00044-016-1636-5) contains supplementary material, which is available to authorized users.

✉ Neni Frimayanti
nenifrimayanti@yahoo.com

- ¹ Department of Chemistry, Faculty of Science, University of Malaya, Lembah Pantai, 50603 Kuala Lumpur, Malaysia
- ² Drug Design and Development Research Group, University of Malaya, 50603 Kuala Lumpur, Malaysia
- ³ Pharmaceutical Design and Simulation Laboratory, School of Pharmaceutical Sciences, Universiti Sains Malaysia, 11800 Penang, Malaysia

relationships for the chalcone compounds with the aid of 2D and 3D-quantitative structure–activity relationship (QSAR) models.

To ascertain the influence of different functional groups on NA inhibition, 33 chalcones with different functionalities were synthesized through Claisen–Schmidt condensation reaction from the corresponding acetophenones and benzaldehydes (Marais et al., 2005). All synthetic compounds were purified by chromatographic method and characterized by using various spectroscopic techniques. The H1N1 neuraminidase inhibitory potency of the synthetic chalcones was tested by using *in vitro* MUNANA assay with DANA (2, 3-didehydro-2-deoxy-*N*-acetylneuraminic acid) as standard inhibitor (Potier et al., 1979).

Material and methods

General procedure for the synthesis of chalcones

All chalcones were prepared *via* standard Claisen–Schmidt reaction. To a solution of the corresponding acetophenone (1 eq) in ethanol (2.5 mL/mmol), sodium hydroxide (3 eq) was added. After 10 min, benzaldehyde (1.2 eq) was added and the solution was stirred at room temperature overnight. After cooling with ice, the reaction mixture was neutralized carefully using 1N hydrochloric acid. The crude mixture was extracted with ethyl acetate, washed with water and brine afforded chalcones (yield 32–92 %) after column chromatography.

Data set preparation

A data set of 33 chalcone-based compounds (Table 1) and percentage of NA inhibition for chalcones studied at 100 mg/mL in Fig. 1 expressed as % inhibition in the range of 6.80–54.0 %. Among these 33 compounds, 22 compounds were used in the training set for model development and 11 compounds were used as a test set for model validation.

2D QSAR modeling

The 2D molecular structures of the ligands were sketched using the Chem Draw 6.0 software (Cambridge Scientific Computing) while Corina in TSAR 3.3 (Accelrys) software packages used to convert the structures into their 3D conformation. The geometries of these molecules were optimized using the Cosmic module of TSAR. The calculation was terminated when the energy difference or the energy gradient becomes smaller than 1×10^{-5} and 1×10^{-10} kcal/mol, respectively. Molecular descriptors were generated using TSAR 3.3 (Accelrys) for each compound. 316 descriptors

were obtained from this calculation. These descriptors were then reduced to a smaller set of descriptors. These set should be information rich but as small as possible.

Correlation matrix was applied to select the best subset of descriptors to be included in the model by eliminating descriptors that are highly correlated with each other. The next step involved the scaling of descriptors which requires thorough manipulation since there may be underlying relationship between these descriptors and it may not be possible to foresee the effects of this process.

The selected descriptors were used to build the QSAR model. In this study, QSAR models were developed using multiple linear regression analysis (MLRA) technique. In this technique, the values for *F*-to-enter and *F*-to-leave were set to 4. Cross-validation analysis was performed using the leave-one-out (LOO) method where one compound is removed from the dataset and its activity is calculated using the model derived from the rest of the dataset. The cross-validated r^2 (CV) and conventional r^2 that resulted in the lowest error of prediction were chosen (Wermuth, 1998). Unless otherwise stated, the default values for the other QSAR parameters were used.

3D-QSAR model and pharmacophore generation

The 3D-QSAR model was carried out using MOE software packed (Chemical Computing Group Inc). This model was developed using 33 compounds in the data set. QSAR model was developed using partial least squares (PLS) technique. The structure of each molecule was sketched using the molecule builder tool in the MOE software and then minimized using MMFF94x force field to a gradient 0.00001 kcal/mol/Å.

Fifteen pharmacophore descriptors were generated and at the same time pharmacophore of the ligands was performed. Feature of the pharmacophore was carried out using pharmacophore query editor tool and the hypothesis for pharmacophore alignment. In this study, the best alignments of pharmacophore were generated using three features, hydrogen bond donor, hydrogen bond acceptor and hydrophobic atom.

The features of this pharmacophore were then used to ensure that 3D-QSAR model is applicable to molecules with the same properties as the pharmacophore alignment, and can be used to predict the biological activities of the unknown compounds.

H1N1 viral neuraminidase MUNANA assay

All chalcones were tested on H1N1 viral neuraminidase by using MUNANA [2'-(4-methylumbelliferyl)- α -D-*N*-acetylneuraminic acid] assay with DANA was used as standard inhibitor. Fresh stock solution (1 mg/mL) of the sample was

Table 1 Structure and activity data of chalcones

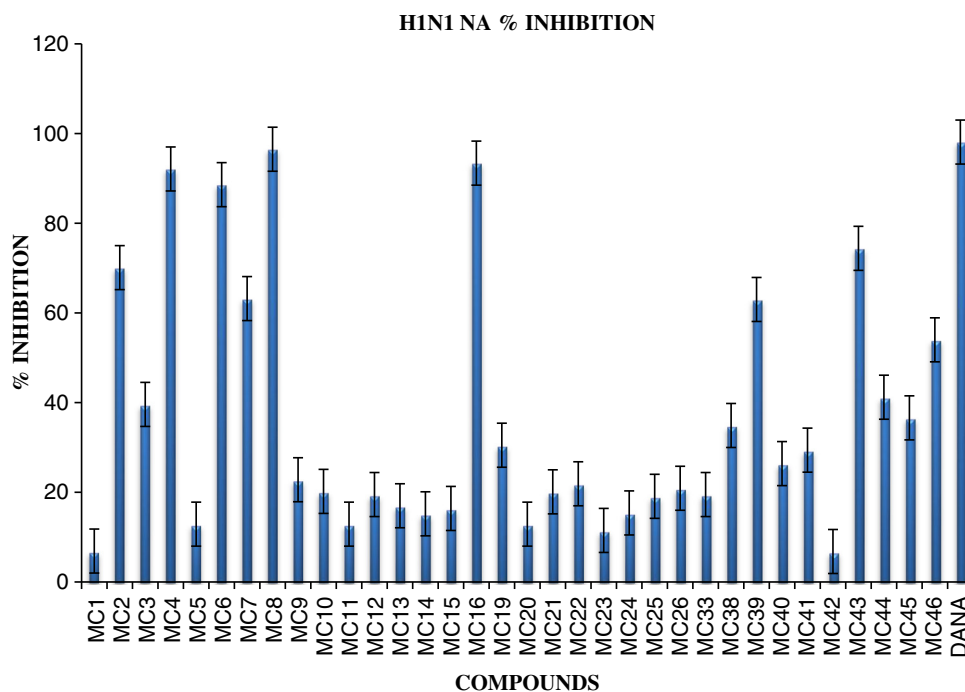
Entry	Compd no	R ¹	R ²	R ³	% of inhibition ^a	Entry	Compd no	R ¹	R ²	R ³	% of inhibition ^a
1	MC1		H	H	6.9	18	MC20		OCH ₃	OCH ₃	12.90
2	MC2		H	H	70.1	19	MC22		OCH ₃	OCH ₃	21.90
3	MC3		H	H	39.60	20	MC23		OCH ₃	OCH ₃	11.50
4	MC4		H	H	92.10	21	MC24		OCH ₃	OCH ₃	15.40
5	MC5		OH	H	12.90	22	MC25		OCH ₃	OCH ₃	19.10
6	MC6		OH	H	60.88	23	MC26		OCH ₃	H	20.90
7	MC7		OH	H	20.63	24	MC33		OCH ₃	H	19.50
8	MC8		OH	H	96.50	25	MC38		NH ₂	H	34.90
9	MC9		OH	H	22.80	26	MC39		NH ₂	H	63.00
10	MC10		OH	H	20.20	27	MC40		NH ₂	H	26.40
11	MC11		OH	H	12.90	28	MC41		NH ₂	H	29.40
12	MC12		OH	H	19.50	29	MC42		NH ₂	H	6.80
13	MC13		OH	H	17.00	30	MC43		H	NH ₂	74.40
14	MC14		OH	H	15.20	31	MC44		H	NH ₂	41.20

Table 1 continued

Entry	Compd no	R ¹	R ²	R ³	% of inhibition ^a	Entry	Compd no	R ¹	R ²	R ³	% of inhibition ^a
15	MC15		OH	H	16.40	32	MC45		H	NH ₂	36.60
16	MC16		OH	OCH ₃	93.40	33	MC46		H	NH ₂	54.00
17	MC19		OCH ₃	OCH ₃	30.50		DANA				98.1

^a Percentage of inhibition at 1 mg/mL

Fig. 1 Percentage of NA inhibition for chalcones studied at 1 mg/mL



prepared in 2.5 % DMSO. Briefly, 25 μ L H1N1 viral neuraminidase (SINO BIO) was added to 25 μ L of sample solution mixed with buffer in a 96-microplate well. A volume of 50 μ L of substrate (MUNANA (SIGMA, M8639) in 32.5 mM MES (SIGMA, M8250) buffer (pH 6.5) was then added and the mixture was incubated at 37 °C. After one hour, formation of 4-methylumbelliferone was immediately quantified fluorometrically on a Modulus Microplate Reader (Turner Biosystem, USA). The excitation wavelength was set at 365 nm and the emission wavelength at 450 nm. Percentage of inhibition was obtained by fitting experimental data to the logistic graph.

Docking of chalcones to H1N1 viral neuraminidase

The docking of all 33 chalcones onto the neuraminidase of A/Brevig Mission/1/1918 H1N1 strain in complex with zanamivir which downloaded from PDB data bank (www.pdb.org, PDB ID: 3B7E) was achieved using Discovery studio 2.5 software packages (Accelrys). Hydrogen atoms were added to the protein and its backbone was minimized. All ligands were minimized.

Docking was performed by using the Cdocker protocol; a grid based molecular docking method that employs CHARMM forcefields. The protein was firstly held rigid

and the ligands were allowed to flex during the refinement. Two hundred ligand conformations were then generated from the initial ligand structure through high temperature molecular dynamic followed by random rotation, refinement with grid based (GRID 1) simulated annealing and a final grid based or full force field minimization. Upon completion of the docking process, conformations with the lowest cdocker energy were then chosen and compared with the standard DANA (active agents against neuraminidase H1N1 with Cdocker energy equal to -46.11 kcal/mol).

Results and discussion

2D QSAR modeling

The best QSAR model developed for the H1N1 inhibition using MLRA technique has an r^2 value of 0.81 and an r^2 (CV) value of 0.65. The equation is:

$$\begin{aligned} \text{Log } 1/\% \text{inhibition} = & -1.06 * \text{kier chiV5 (path)} \\ & + 0.98 * \text{VAMP HOMO} + 0.79 \\ & * \text{VAMP octupole ZZZ} + 2.10 \end{aligned} \quad (1)$$

Table 2 Statistical output and F test value of the multiple linear regression analysis (MLRA) model

Statistical output	Value
Non-cross validated r^2	0.81
Cross validation r^2 (CV)	0.65
F value	27.54
F -probability	1.23e-007
Standard error of estimate (SEE)	0.18
Residual sum of square (RSS)	0.62
Predictive sum of square (PRESS)	1.16

Table 3 Statistical significance of parameter in QSAR equation

Descriptors	Regression coefficient ^a	Jackknife SE ^b	Covariance SE ^c	t value ^d	t Probability ^e
Kier ChiV5 (path)	-1.06	0.20	0.12	-8.59	5.73e-008
VAMP HOMO	0.98	0.049	0.17	5.53	2.43e-005
VAMP octupole ZZZ	0.79-	0.40	0.20	-3.84	0.001

^a The regression coefficient for each variable in the equation

^b Standard error of each regression coefficient derived from a Jackknife procedure on the final regression model

^c Estimate of the standard error of each regression coefficient derived from the covariance matrix

^d Significance of each variable included in the final model

^e Statistical significance for t values

Generally, QSAR model is accepted if it has an r^2 greater than 0.6 and r^2 (CV) greater than 0.5 (Medina-Franco et al., 2005; Frimayanti et al., 2013). This model, therefore, exhibited high prediction value as can be seen from r^2 and r^2 (CV) value.

The cross-validated coefficient r^2 (CV) defines the goodness of prediction whereas the non-cross-validated correlation coefficient (r^2) indicates the goodness of fit of a QSAR model. The F test value stands for the degree of statistical confidence. The statistical output of the MLRA model is presented in Table 2. A cross-validated coefficient of 0.65 was obtained using the 'leave-one-out' cross validation procedure. This value indicates very good internal predictive capability of the developed model.

The model also exhibited a non-cross-validated correlation coefficient of 0.81. The high value of this parameter adds to its usefulness as a predictive tool. The statistical significance of this parameter is listed in Table 3.

A plot of experimental vs. predicted of log 1/% inhibition is shown in Fig. 2. There is no outlier observed in the plot. Hence, the developed QSAR model could be considered to be stable. The calculated inhibition of compounds in the test set re shown in Table 4.

Based on the QSAR model described above, it could be inferred that percentage of inhibition will improve with the increase of the electrostatic parameter (i.e., VAMP octupole ZZZ and VAMP HOMO). The electrostatic parameters are properties of a molecule which are related to its electron affinity and demonstrate its susceptibility towards attack by nucleophiles (Sharma and Kohli, 2014). In this study, VAMP octupole ZZZ and VAMP HOMO correlates well with the percentage of inhibition. As an example, the presence of dimethylamine at R^1 ; hydroxyl group at R^2 and a methoxy group at R^3 of compound **MC16** (93.4 % NA inhibitory activity) increased the electrostatic parameter which promotes the percentage of inhibition.

Topological descriptor (kier ChiV5) calculates the Kier and Hall kappa molecular shape indices which are important descriptors used to define the steric influence of substituents in the interactions of organic compounds with

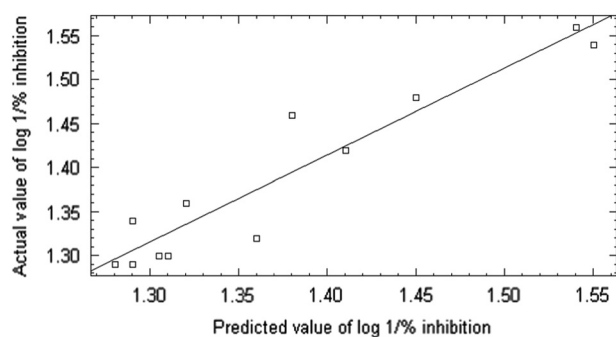


Fig. 2 Plot of actual value vs. predicted value of log 1/% inhibition of compounds in the training set

Table 4 Calculated value of Log 1/% inhibition of chalcone based compounds in the test set based on 2D QSAR model

Entry	Compound No.	Experimental log 1/ % inhibition	Predicted log 1/% inhibition
1	MC45	1.56	1.54
2	MC38	1.54	1.55
3	MC19	1.48	1.45
4	MC41	1.46	1.38
5	MC40	1.42	1.41
6	MC9	1.36	1.32
7	MC22	1.34	1.29
8	MC26	1.32	1.36
9	MC10	1.3	1.30
10	MC12	1.29	1.28
11	MC33	1.29	1.29

macromolecular drug receptor (Praphat et al., 2011). Increasing the value of kier ChiV descriptor will decrease the percentage of inhibition. For example, the bulky naphthalene ring in R¹ of compound **MC42** increased the kier ChiV5 values but showed a diminished NA inhibitory activity (6.8 %).

The percentage of inhibition of the compounds in the test set (i.e., 11 chalcone-based compounds) was predicted using this QSAR model (Eq. 1). The calculated percentage of inhibition values of the compounds in the test set are listed in Tables 4.

The correlation coefficient (r^2) between predicted and experimental value for the QSAR model was also calculated. A predictive correlation coefficient r^2 value (test set) of 0.94 was obtained for the developed QSAR model.

3D QSAR modeling

Pharmacophore features in this study generated 15 types of descriptors. The feature selection was used to select the best descriptors that could be used in the QSAR model. Principle

component analysis (PCA) was applied to reduce the dimensionality of set of molecular descriptors by linearly transforming the data. 3D plot of PCA1, PCA2 and PCA3 is shown in Fig. 3.

3D-QSAR model was then generated using the partial least squares (PLS) technique where the percentage of inhibition served as the dependent variable and the pharmacophore descriptors were used as the independent variable. The resulting model gave a root mean squares error (RMSE) and coefficient correlation (r^2) of 0.204 and 0.71, respectively.

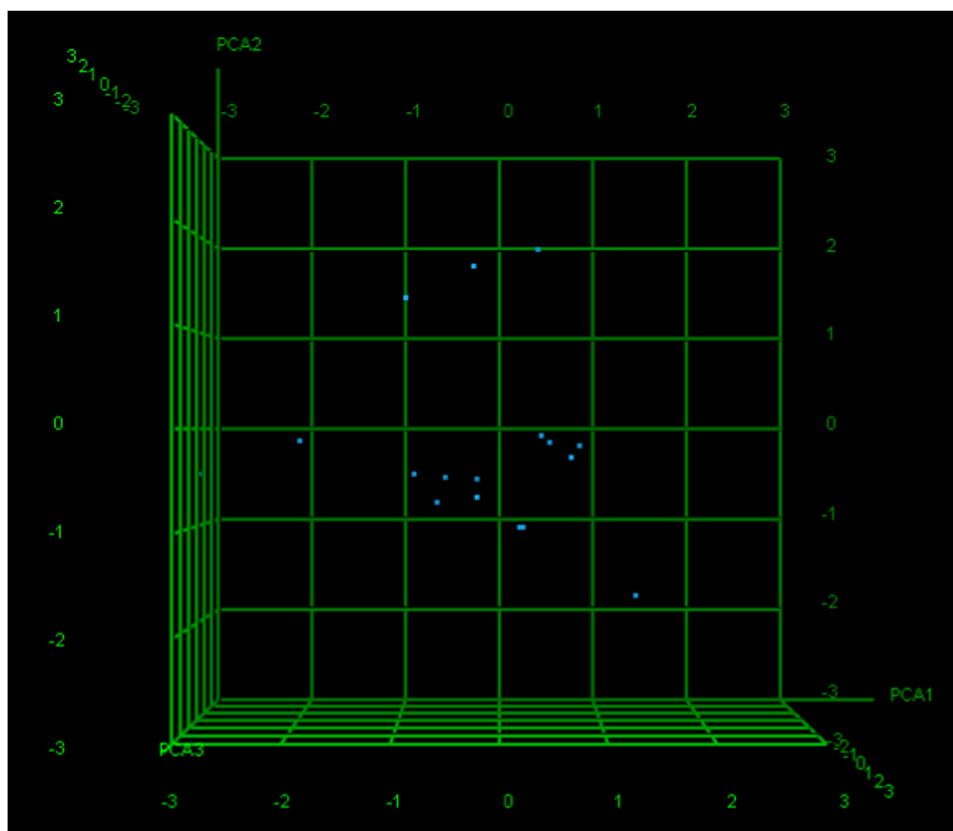
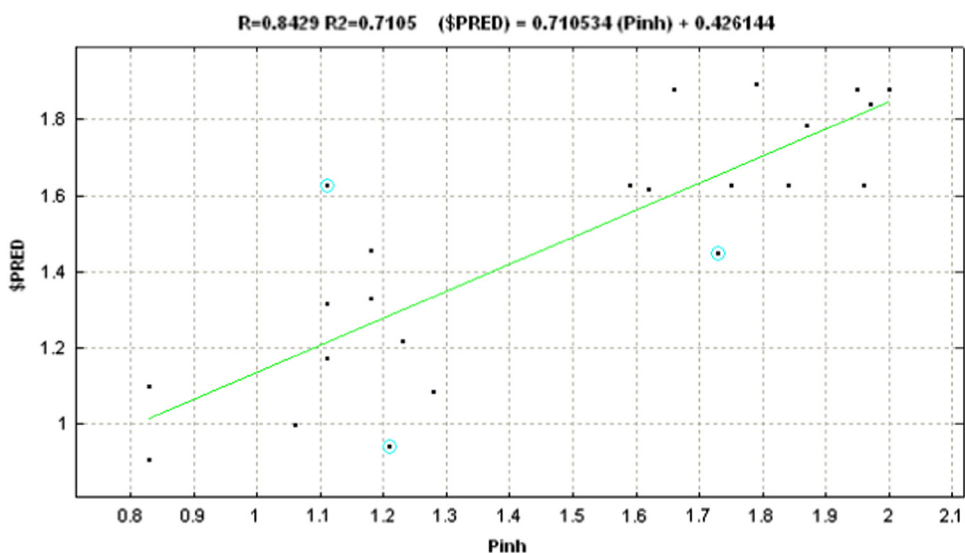
A plot of the actual value of the percentage of inhibition vs. the predicted value of the percentage of inhibition is shown in Fig. 4. The distribution of compounds is observed to be in surrounding region of the linear regression, except for three chalcones (**MC46**, **MC15** and **MC5**) which were seen as outliers (circled in Fig. 4).

The 3D-QSAR model was then validated by predicting the percentage of inhibition of 11 compounds in the test set. The predicted value and actual value of compounds in the test is shown in Table 5. Overall, this 3D-QSAR model is able to predict the biological activity of compounds in the test set with r^2 prediction of 0.51.

The suggested descriptors (in the QSAR model) were then validated using pharmacophore alignment. The training set was aligned on the template using the fit and statistically significant pharmacophore hypothesis for chalcone **MC8** (96.5 % NA inhibition) (Fig. 5). The pink sphere in Fig. 5 is featured for hydrogen bond donor; green sphere for hydrophobic and yellow sphere represented the aromatic ring feature.

A pharmacophore is the ensemble of steric and electronic features that is necessary to ensure the optimal supra-molecular interactions with a specific biological target and to trigger (or block) its biological response (Wermuth, 1998). In addition, the pharmacophore also shows the importance of the hydrophobic, hydrogen bond donor and aromatic ring features in enhancing biological activity. As it shown in Fig. 5, hydrogen bond donor (pink) and hydrophobic sphere (green) were observed in the vicinity of ring A. Thus, it is presumed that compound such as **MC8**, the highest percentage of NA inhibition may be due to the presence of hydroxyl groups in the R¹ and R² positions.

From the result above, it is reasonable to conclude that NA inhibitory action of chalcones can be regulated by multiple mechanisms. To find the possible structure requirement for NA inhibitory activity, meaningful 2D and 3D-QSAR models were derived. 2D-QSAR model indicated that electrostatic parameter may enhance the bioactivity of the chalcone such as **MC16** while steric influence of substituent and probably lack of flexibility such as in chalcone **MC42** may diminish its potency as NA inhibitor.

Fig. 3 3D plot of principle component analysis (PCA)**Fig. 4** Plot of predicted log 1/% inhibition vs. actual log 1/% inhibition of compounds in the training set

3D-QSAR model also showed the importance of the position of the hydroxyl group in A ring which can influence the hydrophobic, hydrogen bond donor and aromatic ring features of the compounds and presumably enhance their biological activities.

Amongst all chalcones, **MC8** showed the best NA inhibitory activity with the percentage of inhibition almost comparable with DANA. The present investigation provides useful information on the structure requirements for the

interaction of chalcones with NA protein in order to ascertain potential directions for synthetic lead-optimization studies.

Docking results

In silico docking studies were performed to evaluate the effects of chalcones against neuraminidase. The Cdocker energy reflects the interaction energy for the ligand-protein

complex. The lower the Cdocker energy means the interaction is more stable. The Cdocker energy is presented in Table 6.

The calculated Cdocker energy for **MC8** and **MC16** showed relatively low value which seems to corroborate with the experimental results. In addition, **MC5** and **MC15** which showed relatively higher Cdocker interaction energy did not show good H1N1 inhibition activities.

MC8 showed to have four hydrogen bonds (blue dashed line) with residue Arg118, Glu227, Arg292 and Arg371. In addition, a π interaction was also found between ligand and residue Arg152 and Arg371. Residues Asp151, Arg152, Glu119, Glu277 and Asn294 showed interaction with the ligand through van der Waals interaction (green cycle) suggesting the importance of these five residues in the formation of van der waals binding pocket. Likewise, in the case of **MC16**, three hydrogen bonds were observed between the ligand and residues Arg118D, Arg292 and Arg374. This ligand displayed π interaction with residues Arg152 and Arg374. The higher the number of the

Table 5 The actual value and predicted value of log 1/% inhibition of compounds in the test set based on 3D QSAR model

Entry	Compound	Actual value of log 1/% inhibition	Predicted value of log 1/% inhibition
1	MC45	1.56	1.61
2	MC38	1.54	1.78
3	MC19	1.48	1.06
4	MC41	1.46	1.68
5	MC40	1.42	1.61
6	MC9	1.36	1.52
7	MC22	1.34	1.27
8	MC26	1.32	1.08
9	MC10	1.3	1.41
10	MC12	1.29	1.54
11	MC33	1.29	0.58

hydrogen bond, may accounts for ligand is more active (Mahto et al., 2012).

However, **MC5** with only one hydrogen bond (between hydroxyl group of the ligand and residue Arg152) and a π interaction with the residue Arg292 showed relatively high Cdocker energy and less inhibition. The binding interaction for **MC5**, **MC8** and **MC16** are illustrated in Fig. 6

Combined inhibitory activity and docking studies suggested that in the presence of hydroxyl groups in the R1 and R2 positions in **MC8** and **MC 16** may fill better into the adjunct pockets resulting more number of hydrogen bond-

Table 6 The Cdocker interaction energies of chalcone derivatives with neuraminidase

Entry	Compound	(-) Cdocker interaction energy(kcal/mol) ^a	Entry	Compound	(-) Cdocker interaction energy(kcal/mol) ^a
1	MC1	28.25	18	MC20	37.21
2	MC2	31.80	19	MC22	38.58
3	MC3	35.69	20	MC23	39.28
4	MC4	29.74	21	MC24	38.12
5	MC5	28.08	22	MC25	35.31
6	MC6	36.94	23	MC26	35.31
7	MC7	33.04	24	MC33	33.82
8	MC8	36.94	25	MC38	31.74
9	MC9	35.35	26	MC39	31.60
10	MC10	38.65	27	MC40	35.85
11	MC11	43.25	28	MC41	35.78
12	MC12	35.41	29	MC42	31.19
13	MC13	32.54	30	MC43	30.32
14	MC14	35.37	31	MC44	27.82
15	MC15	29.25	32	MC45	33.26
16	MC16	43.05	33	MC46	35.29
17	MC19	38.39	34	DANA	46.11

^a Calculation performed using Cdocker (Discovery Studio 2.5, Accelrys)

Fig. 5 The best pharmacophore hypothesis for compound **MC8**, distance between pharmacophore features is reported in Angstrom. Pharmacophores are color coded with yellow for aromatic ring, pink for hydrogen bond donor and green for hydrophobic

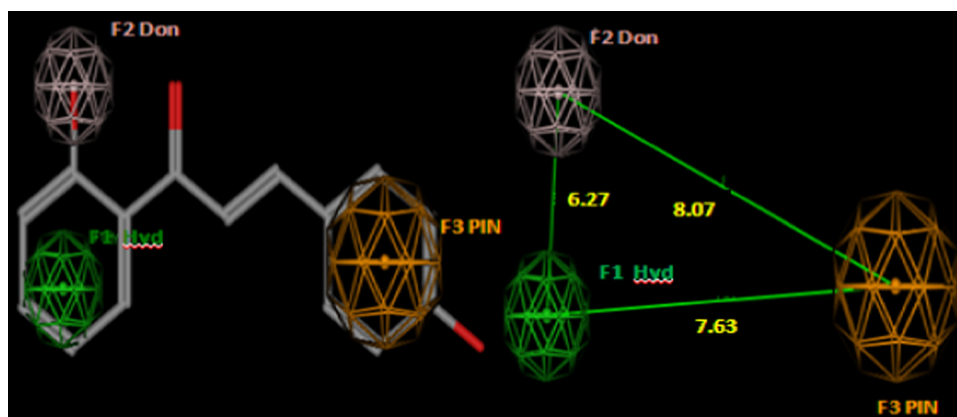
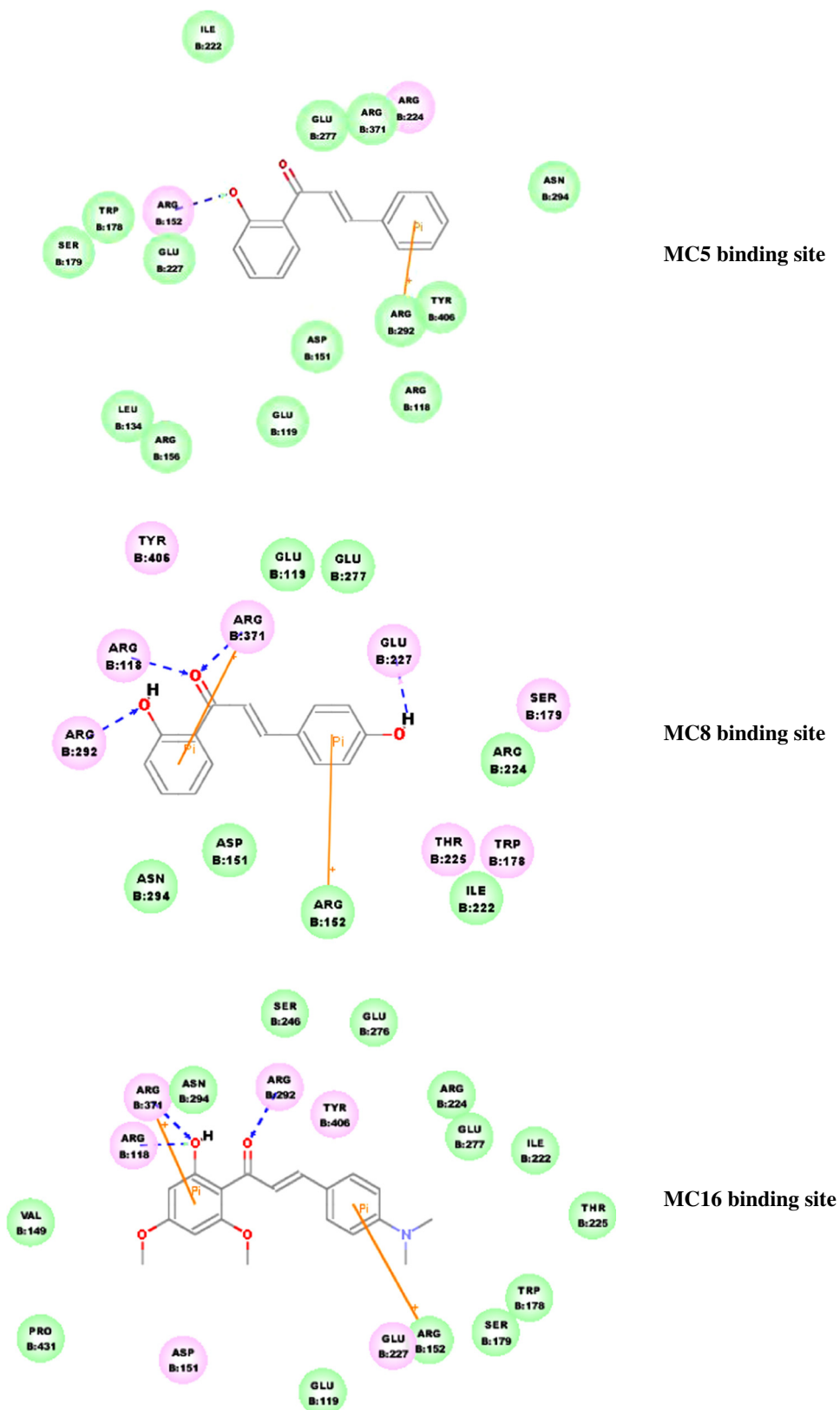


Fig. 6 The binding interaction of MC5, MC8 and MC16



ing and π interactions with the relative residue as Arg118, Arg227, Arg292, Arg371, Arg152, Arg371, Asp151, Arg152, Glu119, Glu277, Asn294 and Arg118D, Arg292, Arg374, Arg152, Arg374, respectively, which can presumably enhance the biological activity of these chalcones.

Conclusion

The 2D and 3D-QSAR model has been successfully developed with a good correlative and predictive ability for predicting neuraminidase inhibitory activity of this chalcone series. Based on 2D-QSAR model, the electrostatic properties can enhance the inhibitory activity. 3D-QSAR model showed that the increasing of the biological activity will be influenced by the hydrogen bond donor, hydrophobic properties and aromatic ring features of the compound. Docking studies were performed to evaluate the effects of chalcones against neuraminidase.

Docking study showed the binding affinity of chalcone derivatives to be within the enzyme binding pockets with relatively less Cdocker interaction energies and higher numbers of hydrogen bonding which validated them as potential candidates for second generation drug discovery.

Bioassay studies of all chalcones indicated that the compounds such as **MC8** and **MC16** bearing hydroxyl groups in the R1 and R2 positions have better biological activities against neuraminidase, suggesting that they are promising as potential inhibitors for H1N1 virus Neuraminidase.

Acknowledgments We thank University of Malaya for the financial support through the project Grant Scheme 53-02-03-1059 and Malaysian Ministry of Science, Technology and Innovation for the H1N1 grant 09-05-IFN-MEB 004.

Compliance with ethical standards

Conflict of interest The authors declare that they have no conflict of interest.

Reference

Babu YS, Chand P, Bantia S, Kotian P, Dehghani A, El- Kattan Y, Lin TS, Hutchison TL, Elliott AJ, Parker CD, Ananth SL, Horn LL, Laver GW, Montgomery JA (2000) BCX-1812 (RWJ-270201):

discovery of a novel, highly potent, orally active, and selective influenza neuraminidaseinhibitor through structure-based drug-design. *J Med Chem* 43:3482–3486

- Frimayanti N, Lee VS, Zain SM, Wahab HA, Rahman NS (2013) QSAR and pharmacophore studies on thiazolidine-4-carboxylic acid derivatives as neuraminidase inhibitors in H3N2 influenza virus. *Med Chem Res* 23(3):1447–1453
- Gao L, Zu M, Wu S, Liu AL, Du GH (2011) 3D QSAR and docking study of flavone derivatives as potent inhibitors of influenza H1N1 virus neuraminidase. *Bioorg Med Chem Lett* 21: 5964–70
- Jeong HJ, Ryu YB, Park SJ, Kim JH, Kwon HJ, Park KH, Rho MC, Lee WS (2009) Neuraminidase inhibitory activities of flavonols isolated from *Rhodiodarosea* roots and their in vitro anti-influenza viral activities. *Bioorg Med Chem* 17: 6816–6823
- Mahto MK, Raj VK, Bhaskar PM, Divya R (2012) ADMET and molecular docking studies of novel zanamivir analogs as neuraminidase inhibitors. *Int J Pharm Sci Rev Res* 13(1):91–94
- Medina-Franco JL, Golbraikh A, Oloff S, Castillo R (2005) Quantitative structure activity relationship analysis of pyridinone HIV-1 reverse transcriptase inhibitors using the k nearest neighbor method and QSAR-based database mining. *J Comput Aided Mol Des* 19:229–242
- Marais JP, Ferreira D, Slade D (2005) Stereoselective synthesis of monomeric flavonoids. *Phytochem* 66:2095–2176
- Mercader AG, Pomilio AB (2010) QSAR study of flavonoids and biflavonoids as influenza H1N1 virus neuraminidase inhibitors. *Eur J Med* 45:1724–1730
- Potier M, Mameli L, Belisle M, Dallaire L, Melancon SB (1979) Fluorometric assay of neuraminidase with a sodium (4-methylumbelliferyl- α -Image -N-acetylneuraminate) substrate. *Anal Biochem* 94:287–296
- Praphat K, Preeti S, Singh JS (2011) Topological based QSAR study of benzamine as inhibitor of trombin. *J Chem Pharm Res* 3(4):396–303
- Ryu YB, Curtis-Long MJ, Kim JH, Jeong SH, Yang MS, Lee KW, Le WS, Park KH (2008) Pterocarpan and flavanones from *Sophoraflavescens* displaying potent neuraminidase inhibition. *Bioorg Med Chem Lett* 18:6046–6049
- Ryu YB, Curtis-Long MJ, Lee JW, Ryu HW, Kim JY, Lee WS, Park KH (2009) Structural characteristics of flavanones and flavones from *Cudratriaticuspidata* for neuraminidase inhibition. *Bioorg Med Chem Lett* 19:4912–4915
- Ryu YB, Kim JH, Park SJ, Chang JS, Rho MC, Bae KH et al. (2010) Inhibition of neuraminidase activity by polyphenol compounds isolated from the roots of *Glycyrrhiza uralensis*. *Bioorg Med Chem Lett* 20:971–974
- Sharma MC, Kohli D (2014) Insight into the structural requirement of substituted quinazolinone biphenyl acylsulfonamides derivatives as Angiotensin II AT₁ receptor antagonist: 2D and 3D QSAR approach. *J Saudi Chem Soc* 18(1):35–45
- Wermuth CG (1998) Glossary of term used in medicinal chemistry. *Pure Appl Chem* 70:1129–1143